Investigating heterogeneous nucleation in peritectic materials via the phase-field method

2006 J. Phys.: Condens. Matter 18 11121

(http://iopscience.iop.org/0953-8984/18/49/006)

INSTITUTE OF PHYSICS PUBLISHING JOURNAL OF PHYSICS: CONDENSED MATTER

J. Phys.: Condens. Matter **18** (2006) 11121–11129 doi:10.1088/0953-8984/18/49/006

Investigating heterogeneous nucleation in peritectic materials via the phase-field method

Heike Emmerich and Ricardo Siquieri

Computational Materials Engineering, Center of Computational Engineering Science and Institute of Minerals Engineering, RWTH Aachen, Mauerstrasse 5, D-52064 Aachen, Germany

E-mail: siquieri@ghi.rwth-aachen.de

Received 18 July 2006, in final form 19 October 2006
Published 22 November 2006
Online at stacks.iop.org/JPhysCM/18/11121

Abstract

Here we propose a phase-field approach to investigate the influence of convection on peritectic growth as well as the heterogeneous nucleation kinetics of peritectic systems. For this purpose we derive a phase-field model for peritectic growth taking into account fluid flow in the melt, which is convergent to the underlying sharp interface problem in the *thin interface limit* (Karma and Rappel 1996 *Phys. Rev.* E **53** R3017). Moreover, we employ our new phase-field model to study the heterogeneous nucleation kinetics of peritectic material systems. Our approach is based on a similar approach towards homogeneous nucleation in Gránásy *et al* (2003 *Interface and Transport Dynamics (Springer Lecture Notes in Computational Science and Engineering* vol 32) ed Emmerich *et al* (Berlin: Springer) p 190). We applied our model successfully to extend the nucleation rate predicted by classical nucleation theory for an additional morphological term relevant for peritectic growth. Further applications to understand the mechanisms and consequences of heterogeneous nucleation kinetics in more detail are discussed.

(Some figures in this article are in colour only in the electronic version)

1. Introduction

In modelling nucleation it is essential to realize that the solid–liquid interface is known to extend to several molecular layers. This has successively been indicated by experiments [3], computer simulations [4], and statistical mechanical treatments based on the density functional theory [5]. The need to pay particular attention to this diffuse interface results from the fact that for nucleation the typical size of critical fluctuations is comparable to the physical thickness of the interface. The success of such careful treatment can be seen in modern nucleation theories for homogeneous nucleation, which do consider the molecular scale diffuseness of the interface.

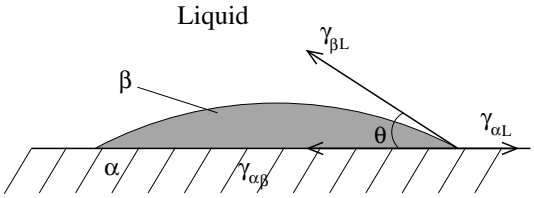

Figure 1. Heterogeneous nucleation of a 'spherical cap'-shaped second phase β on a planar initial phase α according to the 'spherical cap' model. Figure following [9].

These theories could remove the many orders of magnitude difference seen between nucleation rates from the classical sharp interface approach and experiment [6].

In heterogeneous nucleation we face an even more complex situation, since the principal degrees of freedom of the process are larger than in homogeneous nucleation: first of all, each phase can nucleate separately. Moreover, several phases can nucleate jointly, i.e. approximately at the same space and time. Finally one phase can nucleate on top of the other.

Here we are particularly interested in peritectic material systems. Even though many industrially important metallic alloy systems as well as ceramics are peritectics, much less is known about microstructural pattern formation in peritectic growth [7] than, for example, in eutectic growth. Similarly to a eutectic system, the phase diagram of a peritectic system contains a point—the peritectic point with peritectic temperature T_p—at which two different solid phases, the parent (primary) and peritectic (secondary) phases, coexist with a liquid of higher composition than either solid phase. Above T_p, the parent phase is stable and the peritectic phase is meta-stable, whereas below T_p, the opposite is true. In the following, we will consider C to be the concentration of the impurity and T_m the melting point of the pure phase. For a figure displaying a respective schematic phase diagram of a peritectic material system, the reader is refered to [8], for example.

In such peritectic material systems it is particularly relevant to understand the nucleation of the peritectic phase on top of the properitectic phase in detail, since this is the nucleation process yielding the stationary growth morphology. For this specific nucleation process the precise configuration of the properitectic phase, i.e. its free energy on the one hand and its morphology on the other [10], should contribute to the precise nucleation rate.

Nevertheless, the well-established spherical cap model for the nucleation of a new phase β on a planar front of initial phase α predicts the following nucleation rate:

$$I = I_0 \mathrm{e}^{-\Delta F^*/k_\mathrm{B}T}, \tag{1}$$

where I_0 is a constant factor (with dimension equal to the number of nucleations per unit volume and unit time) and ΔF^* is the activation energy for heterogeneous nucleation. Assuming the critical nucleus of phase β to be spherical (see figure 1), the interfacial tensions $\gamma_{\alpha L}$, $\gamma_{\alpha\beta}$ and $\gamma_{\beta L}$ balance each other, enclosing a contact angle θ if the following condition is fulfilled:

$$\gamma_{\alpha L} = \gamma_{\alpha\beta} + \gamma_{\beta L}\cos\theta. \tag{2}$$

ΔF^* is then given, respectively, in two and three dimensions by

$$\Delta F^* = \begin{cases} \dfrac{\gamma_{\beta L}^2}{\Delta F_\mathrm{B}} \times \dfrac{\theta^2}{\theta - (1/2)\sin 2\theta}, & \text{2D} \\ \dfrac{\gamma_{\beta L}^3}{\Delta F_\mathrm{B}^2} \times \dfrac{16\pi(2+\cos\theta)(1-\cos\theta)^2}{12}, & \text{3D.} \end{cases} \tag{3}$$

Here ΔF_{B} is the difference between the bulk free energies of the peritectic phase and of the liquid phase.

Equation (3) determines the classical local nucleation rate and hence the probability per unit time of a nucleus forming as a function of the local temperature at the solid–liquid interface. Thus morphological and energetic contributions to (3) resulting from the properitectic microstructure as discussed in [10] are neglected classically. In the following, we derive for the first time a phase-field model approach for peritectic growth, taking into account hydrodynamics in the molten phase, which is capable of treating this open issue. The way we proceed here is different from the further scientific advance of the authors of [1] in the sense that we analyse the nucleation rate belonging to a heterogeneous nucleation event. In contrast, the authors of [1] extended their own work to investigate several stochastically initialized homogeneous nucleation events of different phases and their subsequent growth in multi-phase systems [11].

Here we will describe our new approach to investigate the rate of a nucleation event of a second phase on top of a first one in detail in section 2. Also, in sections 2 and 3 we investigate microstructure growth in a peritectic system under the influence of hydrodynamic convection in the melt. We will then report on first numerical investigations of the nucleation kinetics in such peritectic material systems, in particular on a morphological contribution from the properitectic phase to (3), in section 3. Moreover, we will discuss the relation of our results to classical nucleation theory in section 3. Finally, we will conclude with a discussion of the general impact of our new approach for peritectic materials under the influence of convection, as well as an outlook.

2. A quantitative phase-field model for peritectic growth taking into account hydrodynamic convection in the molten phase

The starting point of our phase-field modelling approach for heterogeneous nucleation is the free-energy functional of a representative volume of the investigated material system. This free-energy functional is given by the volume integral

$$\mathcal{F} = \int_V f \,\mathrm{d}V, \tag{4}$$

with the free-energy density defined as

$$f = \frac{W(\theta)^2}{2} \sum_i (\nabla p_i)^2 + \sum_i {p_i}^2 (1 - p_i)^2 + \tilde{\lambda} \left[\tfrac{1}{2} \left[c - \sum_i A_i(T) g_i(\vec{p}) \right]^2 + \sum_i B_i(T) g_i(\vec{p}) \right], \tag{5}$$

where $W(\theta) = W_0(1 + \epsilon_4 \cos 4\theta)$ depends on the orientation of the interface, with $\theta = \arctan \partial_y p_i / \partial_x p_i$, ϵ_4 being the measure of the anisotropy and $\tilde{\lambda}$ being a constant. The function g_i couples the phase-field to the concentration and the temperature,

$$g_i = \frac{{p_i}^2}{4} \{15(1 - p_i)[1 + p_i - (p_k - p_j)^2] + p_i(9{p_i}^2 - 5)\}.$$

The coefficients $A_i(T)$ and $B_i(T)$ define the equilibrium phase diagram [2],

$$A_i(T) = c_i \mp (k_i - 1)U, \qquad A_L = 0,$$
$$B_i(T) = \mp A_i U \qquad B_L = 0,$$

where $U = (T_{\mathrm{p}} - T)/(|m_i|\Delta C)$ is the dimensionless undercooling, k_i are the partition coefficients, and A_L, B_L are the corresponding liquid coefficients.

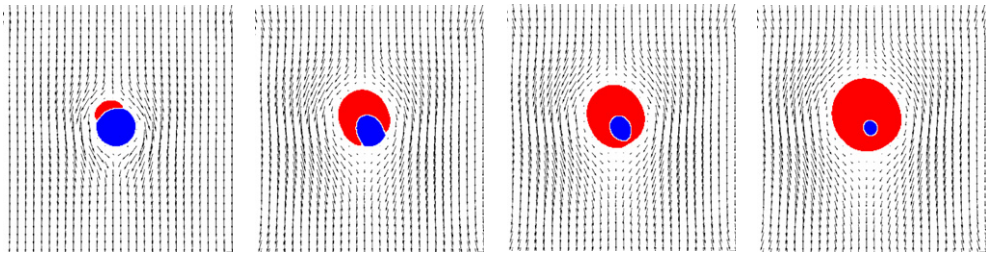

Figure 2. Investigation of the peritectic transformation under the influence of convection. The dark circle indicates the properitectic phase and the light structure the peritectic phase, which is nucleating on top of the properitectic phase. Arrows are vectors indicating the velocity of the hydrodynamic field in the molten phase.

We use three phase fields $p_i \in [0, 1]$, where $\sum_{i=1}^{3} p_i = 1$. The p_i label the properitectic, the peritectic and the liquid phase, respectively, i.e. $i = \alpha$ (for the properitectic phase), $i = \beta$ (for the peritectic phase) and $i = L$ (for the liquid phase); denote $\vec{p} \equiv (p_\alpha, p_\beta, p_L)$.

Their dynamics are derived from the free-energy functional $\mathcal{F}$:

$$\frac{\partial p_i}{\partial t} = \frac{1}{\tau}\frac{\delta \mathcal{F}}{\delta p_i},$$

where τ is a relaxation time.

The concentration field is given by:

$$\frac{\partial c}{\partial t} + p_L \mathbf{v} \cdot \vec{\nabla} c - \vec{\nabla} \cdot \left(M(p_i) \vec{\nabla} \frac{\delta \mathcal{F}}{\delta c} - \vec{J}_{\mathrm{AT}} \right) = 0, \tag{6}$$

where $M(p_i)$ is a mobility and $\vec{J}_{\mathrm{AT}}$ is the anti-trapping term. The scaled concentration field is given by $c_i = (C_i - C_{\mathrm{p}})/\Delta C$, where C_{p} is the liquidus concentration at T_{p}. The model equations so far—except for the anisotropic form of W, which we apply here in the context of these equations for the first time—were developed initially in [2]. In the following, we extend these equations to also model hydrodynamic transport in the liquid phase. This requires their coupling to an additional hydrodynamic field equation, which we realized as follows:

$$\frac{\partial p_L \mathbf{v}}{\partial t} = -p_L \mathbf{v} \cdot \vec{\nabla} \mathbf{v} - p_L \vec{\nabla} \mathbf{p} + \frac{1}{Re} \nabla^2 p_L \mathbf{v} + M_1^2. \tag{7}$$

Equation (7) is a modified Navier–Stokes equation, where $Re = \frac{\rho U}{\nu}$. M_1^2 is a dissipative interfacial force per unit volume and is modelled as in [20].

To our knowledge, this is the first phase-field model convergent to the underlying sharp interface problem in the thin interface limit. The respective asymptotic analysis is summarized in [21]. This model allows us for the first time to investigate quantitatively the peritectic transformation under the influence of convection. A representative evolution is depicted in figure 2, where time runs from the upper left picture to the upper right and the lower left to the lower right. The light circle indicates the properitectic phase and the dark structure the peritectic phase, which is nucleating on top of the properitectic phase. Comparing peritectic growth with and without convection, we find that hydrodynamic transport in the melt enhances the growth process considerably. This relation between melt flow and solidification dynamics is summarized in figure 3, where two pictures of growing microstructures are given at the same set of parameters, except that the right microstructure is subject to flow whereas, to the left, growth proceeds in a purely diffusion limited way. These results are in qualitative agreement with experimental investigation of the peritectic material system Nd–Fe–B in [14].

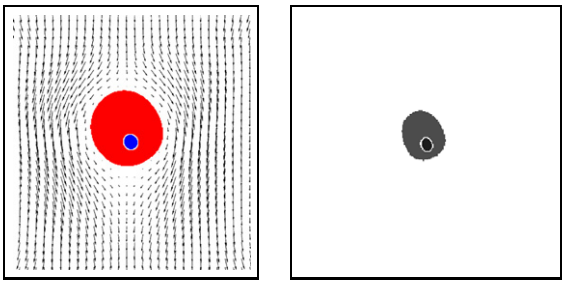

Figure 3. Comparison of peritectic growth with and without convection.

3. Investigating heterogeneous nucleation in peritectic materials via the phase-field method

In solidification experiments the final microstructure is determined by both the peritectic growth dynamics as well as the microstructure growth kinetics. Therefore, for a full quantitative comparison with experiments, it is essential to analyse the heterogeneous nucleation kinetics of the above peritectic material system as well. For such a system, a nucleation event arises as a critical fluctuation, which is a non-trivial time-independent solution of the governing equations that we can derive from the underlying free-energy functional. Our derivation follows the standard variational procedure of phase-field theory (for a review, see e.g. [15–17]). Solving the equations (4)–(7) numerically under boundary conditions that prescribe bulk liquid properties far from the fluctuations ($p_i \rightarrow 1$, and $c \rightarrow c_\infty$ at the outer domain boundaries) and zero field-gradients at the centre of the respective phases, one obtains the free energy of the nucleation event as

$$\Delta F^* = F - F_0. \tag{8}$$

Here F is obtained by evaluating numerically the integration over F after having the time-independent solutions inserted, while F_0 is the free energy of the initial liquid. The zero field gradients arise naturally due to the stationarity of the problem if the 'seed' phase is chosen to be large enough[1]. Based on (8), the homogeneous nucleation rate is calculated as

$$I = I_0 \exp\{-\Delta F^*/kT\}, \tag{9}$$

where the nucleation factor I_0 of the classical kinetic approach is used, which proved consistent with experiments [18].

As introduced in section 1, in a peritectic material sample it is particularly relevant to understand the nucleation of the peritectic phase on top of the properitectic phase in detail, since this is the nucleation process yielding the stationary growth morphology. As demonstrated previously via analytical predictions and Monte Carlo studies (see e.g. [10, 13]), for this specific nucleation process the precise configuration of the properitectic phase, i.e. its free energy on the one hand and its morphology on the other, should contribute to the precise nucleation rate. This, as well as experimental evidence for deviations from classical nucleation theory in the system Nd–Fe–B [19], motivated us to study the effect of two morphological features of the properitectic phase on the nucleation rate of the peritectic phase, namely (I) the effect of facets and (II) the effect of its radius. In this context, the underlying facetted shape of the properitectic

[1] Thermodynamically, this is always possible. The functioning of the underlying relaxation procedure does not depend on the volume of the properitectic phase as such, but on the relative volume of the properitectic phase to the volume that we choose as the initialization for the peritectic phase. This has to be tuned close to a ratio to be expected from the position in the phase diagram to ensure convergence within the limit of a reasonable number of variations.

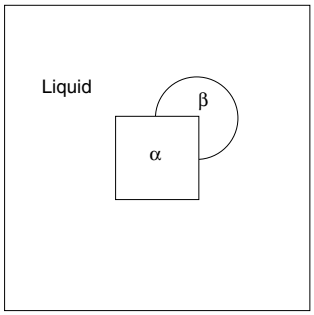

Figure 4. Schematic sketch to elucidate the initialization of the relaxation procedure and subsequent calculation to determine the heterogeneous nucleation rate via the phase-field method for the case of an anisotropic 'seed'.

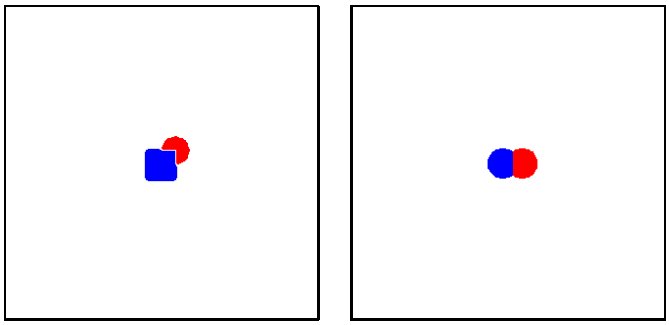

Figure 5. Possible morphologies of the critical 'two-phase' nucleus for an anisotropic and an isotropic underlying properitectic 'seed', respectively. The parameters used in the phase-field model equations to result in these mophologies were: $m_\alpha = -3.73$ K/at.%, $m_\beta = -0.6$ K/at.%, $T_\mathrm{p} = 1790.4$ K, $D = 5.0 \times 10^{-9}$ m^2 s^{-1} and the scaled concentrations $c_\alpha = -2.16$ and $c_\beta = -1.16$.

phase is initialized as a 'seed' for the peritectic phase to nucleate on, as depicted in figure 4. Figure 4 reveals, too, that in our investigations the peritectic phase is nucleating at the corner of the properitectic phase. To calculate the nucleation rate of the peritectic phase on top of this facetted seed, it is then—as described above—essential to determine the corresponding time-independent configuration, at which neither of the two phases will grow, and at which also all diffuse fields are fully relaxed, i.e. stationary. To find this state, we vary the radius of the properitectic phase systematically, keeping the position of its centre relative to the properitetic phase constant. For each variation, we carry out the relaxation procedure. There is exactly one radius, where stationarity can be achieved, namely the radius of the critical nucleus. The precise morphology of the critical 'two-phase' nucleus, in particular the ratio of the volume of the two phases, depends—as indicated above—on the precise thermodynamic state of the system under investigation, as can easily be understood from the phase diagram. Such possible heterogeneous nuclei for the parameter settings given underneath are depicted in figure 5 for an anisotropic 'seed' and an isotropic underlying properitectic 'seed', respectively. The anisotropic form $W(\theta) = W_0(1 + \epsilon_4 \cos 4\theta)$ for $W(\theta)$ allows us to obtain this state for the anisotropic case. However, we are aware that, for a simulation of the full dynamic microstructure evolution into a facetted shape, more elaborate anisotropic forms of $W(\theta)$ are required, as, for example, given in [22].

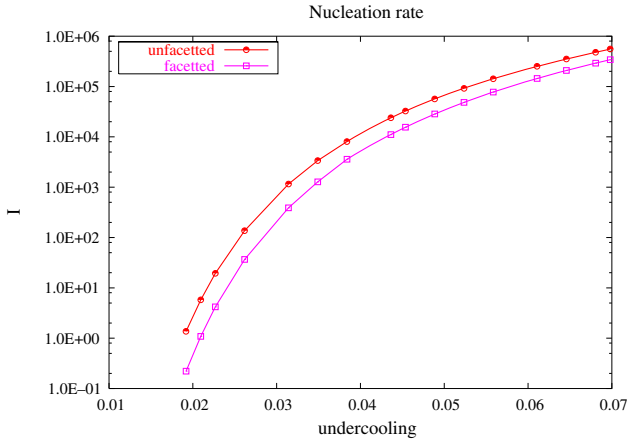

Figure 6. Comparison of the nucleation rate on top of a facetted nucleus to the one on top of an unfacetted nucleus.

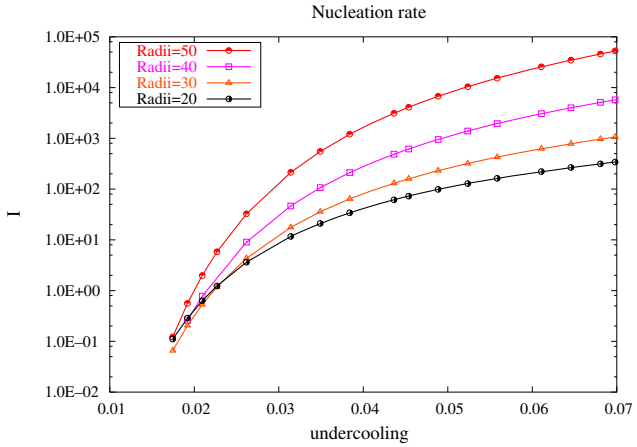

Figure 7. Comparison of the nucleation rate on unfacetted nuclei of different radii.

In figures 6 and 7 we summarize our results. As you can see from figure 6, the less facetted the properitectic phase, the larger the nucleation probability for a peritectic nucleation on top of it. For the contribution resulting from the radius of the properitectic phase, a similar relation is true: the larger the radius of the properitectic phase, the larger the probability of a peritectic nucleation on top of it. Both findings are in qualitative agreement with the following atomistic picture: unfacetted nuclei offer a great number of surface kinks for nucleation. This holds for nuclei of small radii, as well. However, small radius nuclei are also subject to large surface diffusion due to kink flow [12]. This overrides the first effect such that the overall nucleation rate turns out to be smaller for smaller radii. Moreover, these findings are in qualitative agreement with [10] and thus provide a first qualitative validation for our new approach towards heterogeneous nucleation. However, it should be noted that the atomistic picture is just given for a common-sense estimation of what our model should do. In the continuum picture underlying our investigations, the differences in the various curves arise due to the fact that the total surface energy tied to the diffuse surface area of

the properitectic nucleus depends on its morphology. Thus the latter naturally has an impact on the nucleation rate, just as indicated experimentally. This can be analysed in more detail by making use of the phase-field profiles at the stationary point [21]. The benefit of using our continuum model approach rather than atomistic models for the proposed studies is twofold: (1) the approach is computationally considerably more efficient, i.e. it will easily allow for subsequent 3D simulation and simulations of several nuclei competing in the course of initial growth. This also implies that the timescales that can be accessed are larger than for atomistic simulations. Only due to this does simulation of nucleation as well as initial growth become possible. (2) Moreover, it can easily be extended to additional physical mechanisms influencing the nucleation process as, for example, elastic ones [17] or anisotropies of the solid–liquid interfacial free energy [21].

4. Discussion and outlook

To summarize, in this paper we have introduced a new phase-field modelling approach for peritectic growth, taking into account hydrodynamic transport in the molten phase. We apply this approach successfully to investigate the influence of melt flow on the peritectic transformation. Moreover, we employ our model to identify the precise mechanisms of the heterogeneous nucleation kinetics in a peritectic system, i.e. essentially mechanisms beyond classical nucleation theory. In this context, it is important to notice that the new features of our approach to heterogeneous nucleation inherently included are (I) the notion of a diffuse interface as well as (II) long-range interaction effects due to our continuum field approach towards the problem. Based on these features, our model can explain differences between classical nucleation theory and experiments as morphological contributions to the nucleation rate. Moreover, it compares well with careful statistical studies of the effects of long-range interactions. In this sense, it poses a valuable new approach towards heterogeneous nucleation in general, taking into account kinetic, thermodynamic as well as long-range interaction effects, which still have to be developed further.

References

[1] Gránásy L, Pusztai T and Börzsönyi T 2003 *Interface and Transport Dynamics* (*Springer Lecture Notes in Computational Science and Engineering* vol 32) ed H Emmerich, B Nestler and M Schreckenberg (Berlin: Springer) p 190
[2] Folch R and Plapp M 2005 *Phys. Rev.* E **72** 011602
[3] Huisman W J, Peters J F, Zwanenburg M J, de Vries S A, Derry T E, Albernathy D and van der Veen J F 1997 *Nature* **390** 379
[4] Davidchack R L and Laird B B 1998 *J. Chem. Phys.* **108** 9452
[5] Ohnesorge R, Löwen H and Wagner H 1994 *Phys. Rev.* E **50** 4801
[6] Gránásy L and Iglói F 1997 *J. Chem. Phys.* **107** 3634
[7] Boettinger W J, Coriell S R, Greer A L, Karma A, Kurz W, Rappaz M and Trivedi R 2000 *Acta Mater.* **48** 43
[8] Lo T S, Karma A and Plapp M 2001 *Phys. Rev.* E **63** 031504
[9] Porter D A and Easterling K E 1981 *Phase Transformations in Metals and Alloys* 2nd edn (New York: Van Nostrand-Reinhold)
[10] Ain J K 1958 *Growth and Perfection of Crystals* ed R H Doremus, B W Roberts and D Turnbull (New York: Wiley) p 319
[11] Gránásy L, Pusztai T, Tegze G, Warren J A and Douglas J F 2005 *Phys. Rev.* E **72** 011605
Gránásy L, Pusztai T, Börzsönyi T, Warren J A and Douglas F 2004 A general mechanism of polycrystalline growth *Nat. Mater.* advance on-line publication Aug. 8
[12] Pierre-Louis O, D'Orsogna M R and Einstein T L 1999 *Phys. Rev. Lett.* **82** 3661
[13] Shneidman V A, Jackson K A and Beatty K M 1999 *Phys. Rev.* B **59** 3579
[14] Filip O, Hermann R and Schultz L 2004 *J. Mater. Sci. Eng.* A 375

[15] Warren J A and Boettinger W J 1995 *Acta Metall. Mater.* **43** 689
[16] Boettinger W J and Warren J A 1996 *Metall. Mater. Trans.* A **27** 657
[17] Emmerich H 2003 *The Diffuse Interface Approach in Material Science—Thermodynamic Concepts and Applications of Phase-Field Models* (*Springer Monograph, Lecture Notes in Physics* LNPm 73) (Berlin: Springer)
[18] Kelton K F 1991 *Solid State Phys.* **45** 75
[19] Strohmenger J, Volkmann T, Gao J and Herlach D M 2004 *Mater. Sci. Eng.* A **375** 561
Volkmann T, Strohmenger J, Gao J and Herlach D M 2004 *Appl. Phys. Lett.* **85** 2232
[20] Beckermann C, Diepers H-J, Steinbach I, Karma A and Tong X 1999 *J. Comput. Phys.* **154** 468
[21] Emmerich H and Siquieri R 2006 in preparation
[22] Debierre J M, Karma A, Celestini F and Guerin R 2003 *Phys. Rev.* E **68** 041604